FLOW PATTERN AND PRESSURE DROP OF TWO-PHASE FLOW IN A HORIZONTAL DISTRIBUTOR TUBES

AZIZ, A.[*,**], MIYARA, A.[*], SUGINO, F.[*]

[*] Department of Mechanical Engineering, Saga University
1 Honjou-Machi, Saga-shi, 8408502, Japan
miyara@me.saga-u.ac.jp
[**] Department of Mechanical Engineering, Riau University
Kampus Bina Widya, Jl. Subrantas km 12,5, Pekanbaru, 28293, Indonesia
azridjal@yahoo.com

ABSTRACT

To understand flow pattern and pressure drop behavior of two-phase flow in a distributor tubes, a basic study has been carried out by using air and water as working fluids. The distributor consists of one inlet and two outlet tube branches, upper part and lower part respectively. In experiments, the volumetric flow rates of air and water from each outlet branch were measured and the flow pattern was observed by using a high-speed video camera. Numerical analyses are also carried out by using computational fluid dynamics (CFD) by Fluent software. Similar flow pattern has been obtained by the experiment and CFD. The two-phase pressure drops were calculated using an analytical model, and it was compared with the CFD. On the other hand, the two-phase flow deviation ratio of the experiment and CFD showed small difference for the water and large difference for the air. The description of flow pattern by experiment and numerical are agreed well with the flow pattern on Mandhane and Baker flow pattern map. There are some differences in the pressure drop obtained by the analytical model and CFD, and they are increases with the increasing of superficial gas velocity. The pressure drop is biggest at branching part of the distributor, because of sudden enlargement and sudden contraction in branch.

1.   INTRODUCTION

The use of compact heat exchangers in air conditioning and refrigeration systems has become interest for the last two decades. Smaller tubes have been manufactured and used for high performance of condensers and evaporators. The high pressure drop will occur in the small tube. In order to reduce the pressure drop and to obtain a higher heat transfer performance of refrigerant flow, the flow must be distributed into several channels by using a distributor. Although the refrigerant distributor has installed, equally, to distribute the refrigerant flow from the expansion valve into each evaporator channel, non-uniform distribution occurs sometime, and the heat transfer has deteriorated (Yang, C.Y. et al., 2001, Yoshioka, 2008).

The two-phase flow patterns in horizontal small circular tubes have been studied by a number of researchers. The two-phase flow patterns observed in horizontal tubes are complicated by asymmetry of the phases resulted by the influence of gravity and liquid shear. The accepted flow patterns given by many researchers are dispersed bubble, slug, plug (elongated bubble), stratified, wavy, and annular flow. (Yang, C.Y. et al., 2001, Yoshioka 2008, Wong, T.N. et al., 1997, Brennen, C.E., 2005, Wambsganss, M.W. et al., 1991, Massoud, M., 2005, Ghiaasiaan, S.M., 2008, Tong, L.S. et al., 1997, Kandlikar, S.G. et al., 1999). Other flow patterns, such as, slug-wavy, slug-bubbly, wavy-annular, annular-slug, bubbly-plug, slug-bubbly and semi slug, may be considered transitional flow patterns (Theilacker, J.C., 1987, Ghajar, A.J. 2005, Ghajar, A.J. et al., 2010, Wongwises, S., 2006, Azzopardi, B.J., 2010). Baker (1954) and Mandhane et al. (1974) successfully presented a useful map by using superficial gas velocity (U_G) and superficial liquid velocity (U_L) as coordinates. The data base of this flow regime map is primarily air–water mixture. The flow pattern observed in this study for horizontal flow has been confirmed by the map of Mandhane et al. (1974).

In this study, the main objective is to obtain and clarify the characteristics of flow pattern and pressure drop from air-water two-phase flows through the horizontal distributor with upper and lower branches. The flow pattern was observed experimentally using a high-speed video camera and investigated numerically using computational fluid dynamics (CFD) by Fluent software. The two-phase pressure drop was obtained using an analytical model and also investigated with the CFD. The flow rates of each phase flowing in the outlet after

the distributor branches were measured. To understand the behavior of the two-phase flow in the distributor, flow patterns of the air and water flow have been observed by a high-speed camera.

2.   EXPERIMENTAL INVESTIGATION

2.1.   Experimental Apparatus and Uncertainties

Figure 1 shows the experimental apparatus. The components of the apparatus are an air and water supply system, a merging section, a distributor test section, two gas-liquid separators, an air measuring bath, and a water measuring cylinder. Air flow rate and water flow rate before entering to the test section is controlled by using a flow meter. The air and water are mixed in the merging section. Water was supplied by water source in laboratory. Air was supplied from an air-compressor with pressure regulator. The measurement of air and water flow rates at each exit of distributor was taken after the gas-liquid separator. Air flow rate was measured by air measuring bath and water flow rate by water measuring cylinder. The flow visualization and some photograph of flow patterns were captured using high speed video camera (Keyence Motion Analyzing VW-6000) at a shutter speed 1/30.000 second, frame rate per second (fps) at 500 fps, and reproduction speed at 15 fps.
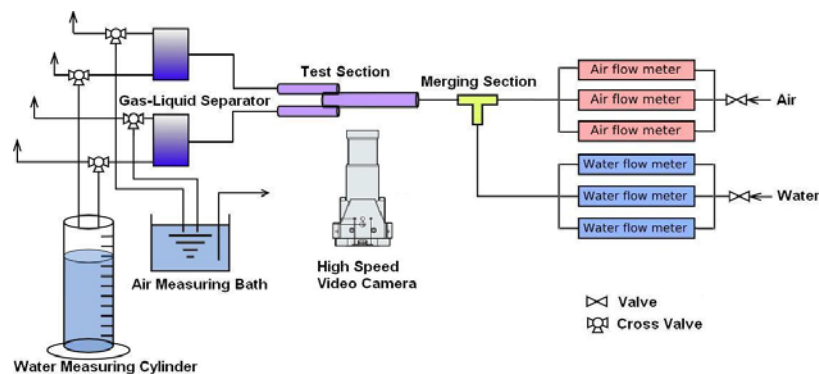

Figure 1. Schematic diagram of experimental apparatus.

The whole test section and the detail of the distributor are shown in Figure 2 and Figure 3, respectively. The test section consists of an entrance tube with a diameter of 8 mm and a distributor with two outlet tubes, upper and lower with a diameter of 5 mm. The entrance tube has 400 mm tube length from the distributor inlet to ensure a fully developed flow. The distributor was machined and polished from a rectangular block of acrylic resin. The transparent block facilitates flow visualization.
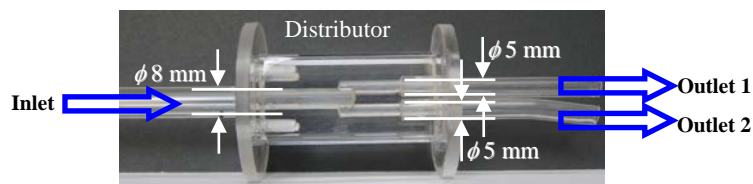

Figure 2. Test Section.

Figure 3. Distributor.

During the whole series of tests, several runs were made to check the repeatability of the data. The data presented are mean values of ten measurements. The error analysis was carried out using the method suggested by Bell (2001) and Moffat (1988). The uncertainties from each measurement is around ±0.5% to

±4.6% for air flow rate and around ±0.3% to ±4% for water flow rate, respectively, where the uncertainties are larger for small flow rate.

2.2. Data Reduction

The air-water volumetric flow rates taken after flow out from the gas-liquid separator are used to evaluate the distributor performance. The volumetric flow rates of air in outlet 1 and outlet 2 are Q_{G1} and Q_{G2}, and the volumetric flow rates of water are Q_{L1} and Q_{L2}, respectively. The non dimensional deviation ratio R is defined with equations (1) and (2). The non dimensional air deviation ratio is R_G, and the non dimensional water deviation ratio is R_L. Where, subscript G is for air and subscript L for water.

$$R_G = (Q_{G1} - Q_{G2})/(Q_{G1} + Q_{G2}) \tag{1}$$

$$R_L = (Q_{L1} - Q_{L2})/(Q_{L1} + Q_{L2}) \tag{2}$$

$R = 1$ indicates that all fluid flows out from the upper outlet, $R = 0$ indicates the equal distribution, and $R = -1$ indicates that all fluid flow out from the lower outlet. The superficial velocities U of each fluid are defined with equations (3) and (4). U_G is the superficial air velocity, and U_L is the superficial water velocity, where, A is flow area of inlet tube.

$$U_G = Q_G/A \tag{3}$$

$$U_L = Q_L/A \tag{4}$$

3. NUMERICAL SIMULATION MODEL

The numerical analysis was performed by using CFD software, Fluent. The three-dimensional distributor with the same shape and dimension of the experimental test section was modelled in GAMBIT with mesh size 0.5 mm, tetrahedral/hybrid scheme. The volume of fluid (VOF) model with double-precision solver was used for calculating unsteady air-water two-phase flow through a distributor. The iteration was bounded up to convergence limit range 0.001. The simulation conditions were set as similar with the experiments. The pressure at the upper and lower outlet of the distributor is atmospheric pressure, and the contact angle is set as 20°. Table 1 shows the physical properties of air and water at atmospheric pressure and on room temperature 20^oC.

Table 1. The physical properties of air and water at atmospheric pressure and on room temperature 20^oC.

Properties	Unit	Air	Water
Density	[kg/m^3]	1.2043	998.21
Viscosity	[kg/(m · s)]	18.206×10^{-6}	1001.6×10^{-6}
Surface tension	[N/m]	0.0721	

4. ANALYTICAL MODEL

The two-phase pressure drop for flows inside tubes are the sum of three contributions: the gravitational pressure drop Δp_{GR}, the acceleration pressure drop Δp_A and the frictional pressure drop Δp_F. So the pressure balance equation is given by:

$$\Delta p_{total} = \Delta p_{GR} + \Delta p_A + \Delta p_F \tag{5}$$

The gravitational pressure drop or head pressure change in the tube is given by:

$$\Delta p_G = \rho_m g \Delta h \tag{6}$$

The acceleration pressure drop Δp_A can be evaluated by the following expression:

$$\Delta p_A = G^2 \left(\frac{1}{\rho_{m,outlet}} - \frac{1}{\rho_{m,inlet}} \right) \tag{7}$$

Where ρ_m is the two-phase mixture density.

Lombardi and Cassana (1992) presented a dimensionless pressure drop correlation for two-phase flow mixtures in vertical ducts. The correlation was compared to experimental pressure drop data in round vertical and inclined tubes, this correlation named CESNEF-2 correlation, the frictional pressure drop is given as:

$$\Delta p_f = \frac{2G_0{}^2}{d\rho_h} \left(f_G b_G + f_L b_L + f_h b_h \right) \Delta L \tag{8}$$

The homogenous density is ρ_h, where f_G, f_L, f_h are the gas, liquid and two-phase friction coefficients, respectively, and b_G, b_L and b_h the corresponding weight functions and d the tube diameter. The gas and liquid friction coefficients f_G and f_L for turbulent flow condition ($Re > 2400$) were calculated by using Colebrook–White correlation, as modified by Selander:

$$f = \frac{1}{\left(3.8 \ln \left(\frac{10}{Re} + 0.2 \frac{\delta}{d} \right) \right)^2} \tag{9}$$

In laminar flow condition ($Re \leq 2400$), f_G and f_L is defined as:

$$f = \frac{16}{Re} \tag{10}$$

In order to calculate f_h (the two-phase friction coefficient) the following equation Lo (dimensionless number) defined as:

$$Lo = \frac{G^2 d}{\sigma \rho_h} \sqrt{\frac{\mu_G}{\mu_L}} \tag{11}$$

Where σ is a surface tension, μ_G and μ_L are the gas and liquid dynamic viscosity, respectively. It was presented that a transition exists in the function of Lo to evaluate f_h for $Lo = 30Ce$, where Ce is a dimensionless number:

$$Ce = \rho_L g \frac{(d - d_o)^2}{\sigma} \frac{\mu_G}{\mu_L} \tag{12}$$

Where d_o is an empirical number equal to $d_o = 0.001$ m, Ce is assumed to be zero for $d < d_o$ and for $Lo \geq 30Ce$ f_h used as:

$$f_h = 0.046 Lo^{-0.25} \tag{13}$$

For $Lo < 30Ce$, f_h defined as:

$$f_h = 0.046 (30Ce) Lo^{-1.25} \tag{14}$$

The pressure change in the junction between inlet and outlet tube is caused by the momentum change due to the turning of the fluid into an upper and lower outlet, respectively, the equation was calculated as follows (Saba and Lahey, 1984):

$$(\Delta P_{0-2})_j = \frac{1}{2} \left(G_0^2 \left(\frac{x_0^2}{\alpha_0 \rho_G} + \frac{(1 - x_0)^2}{(1 - \alpha_0) \rho_L} \right) - G_2^2 \left(\frac{x_2^2}{\alpha_2 \rho_G} + \frac{(1 - x_2)^2}{(1 - \alpha_2) \rho_L} \right) \right) \tag{15}$$

$$\alpha = \left[1 + \left(\frac{1-x}{x} \right)^{1} \left(\frac{\rho_G}{\rho_L} \right)^{0.67} \right]^{-1} \qquad (16)$$

Where void fraction α, was calculated by following correlation by Zivi (1964).

5. RESULT AND DISCUSSION

5.1. Flow Patterns

The observed flow patterns are plotted using superficial water and air velocities on Mandhane (1974) and Baker (1954) flow patterns as shown in Figure 4, where in this paper point f, g and h (oval circle) are discussed, for other points, the flow pattern and flow deviation has been reported in elsewhere. The experiments were carried out on the condition of the superficial water velocity (U_L) setting constant with changing conditions of superficial air velocity (U_G) from low to high or vice versa. Experimental data have been obtained under the conditions of superficial air and water velocities, which are 0.06, 0.15, 0.71 m/s for air and around 0.83 m/s for water, respectively.
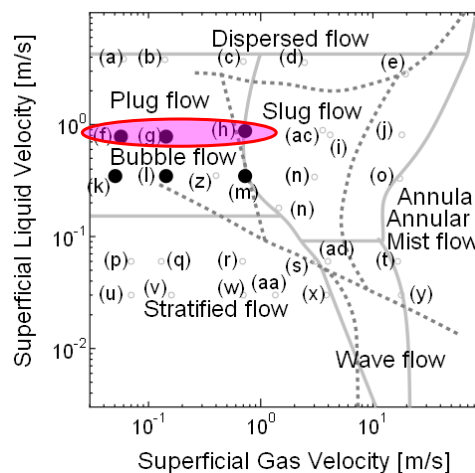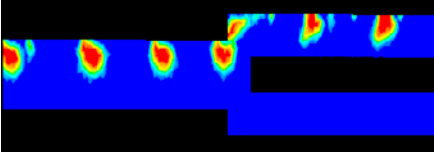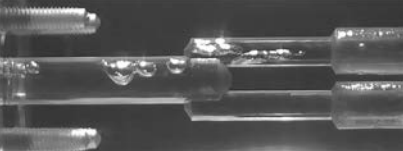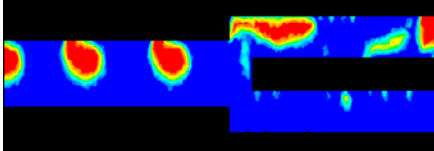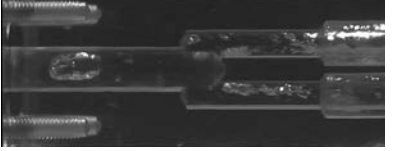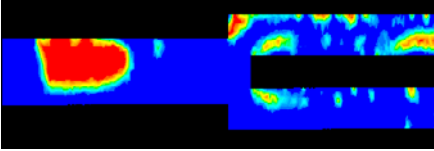

Figure 4. Experimental data point at Mandhane and Baker maps for horizontal flow.

Table 2. Comparison of flow pattern image in distributor for point f, g, and h at U_G from low to high and U_L relatively constant at horizontal position.

Experimental Result	Numerical Simulation	Point
Elongated bubble flow	Elongated bubble flow	Point f U_G = 0.06 m/s U_L = 0.83 m/s
Elongated bubble flow	Elongated bubble flow	Point g U_G = 0.15 m/s U_L = 0.81 m/s
Elongated bubble flow	Elongated bubble flow	Point h U_G = 0.71 m/s U_L = 0.83 m/s

In the experiment for point f, g and h, the developed two-phase flows which are achieved before the distributor, agree to this flow pattern maps. The experiments cover stratified flow, wavy flow, bubble flow, plug flow (elongated bubble flow), dispersed flow, slug flow, and annular flow. Identification of the flow patterns were carried out using flow patterns suggested by Theilacker (1987) and Azzopardi (2010).

The comparison of flow pattern image by experimental and CFD in horizontal distributor position are shown in Table 2, that corresponding with point f, g, and h. Where, the air superficial velocity U_G is varied from low to high (0.06 m/s to 0.71 m/s), and water superficial velocity U_L is kept relatively constant at 0.83 m/s. It showed that the experimental flow patterns tend to have similar patterns with CFD.

The flow pattern cover elongated bubble flow for low to high superficial air velocity. It is similar to elongated bubble flow pattern compared to other references. (Azzopardi, B.J., 2010; Ghajar, A.J., 2005; Massoud, M., 2005; Ghiaasiaan, S.M., 2008). As seen in Table 2 with a gradual increasing of the superficial air velocity, the elongated bubble for both experimental result and CFD are also increasing from small to large elongated bubble, although there is the difference of the flow pattern in distributor by experimental and CFD that affect to the two-phase flow deviation ratio (R_G and R_L) as seen in Figure 5.
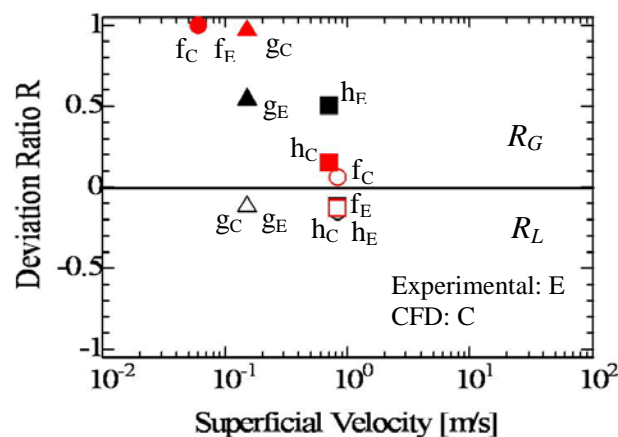

Figure 5. Superficial velocity and deviation ratio for point f, g and h

Figure 5 shows the deviation ratio for point f, g, and h at the superficial velocity for air and water with, which are subscript E for experimental and subscript C colour for CFD, respectively. There is a small difference in deviation ratio R for water between the experimental and CFD, especially at the point f and large difference for air especially at the point g and h. On the other hand, the deviation ratio R both experimental and CFD are similar at the point g and h for water, and at the point f for air.

5.2. Two-Phase Pressure Drop

Figure 6 shows the pressure drop in the horizontal distributor that correlated with point f, g, and h. where the superficial air velocity is varied from low to high (0.06 m/s to 0.71 m/s) and superficial water velocity is kept relatively constant around 0.82 m/s for both CFD and analytical data.

With the same superficial water velocity, the pressure drop increases with increasing superficial air velocity because the friction pressure drop more dominant by increasing superficial air velocity. It is similar to the previous results obtained by various researchers (Wongwises, S., et al., 2006; Saisorn, S., et al., 2008).

The pressure by an analytical model and CFD quite similar although there is some difference pressure drop with the increasing of superficial air velocity as seen in Figure 6. The high pressure drop was occurred in the branching part of the distributor it is caused by the momentum change due to sudden enlargement and sudden contraction from the turning of the fluid into an upper and lower outlet, respectively.

Figure 7 shows the pressure drop comparison for both analytical and CFD in the horizontal distributor at point f, g and h where the superficial air velocity is varied from low to high (0.06 m/s to 0.71 m/s) and

superficial water velocities are kept relatively constant around 0.83 m/s. The pressure drop at superficial water velocity around 0.83 m/s is also increasing with varying superficial air velocity from low to high. This is because, when the superficial water velocity increase with increasing superficial air velocity, the air at elongated bubble flow is more replaced by gas as shown in Table 2 and the air velocity is more than enough to induce water in turbulence and the friction will cause the pressure drop begin to rise again. It is similar to the previous results obtained by various researchers (Wongwises, S., et al., 2006; Saisorn, S., et al., 2008). However, when the water and air velocity increase until the flow are sufficiently turbulent, the pressure drop increase too.
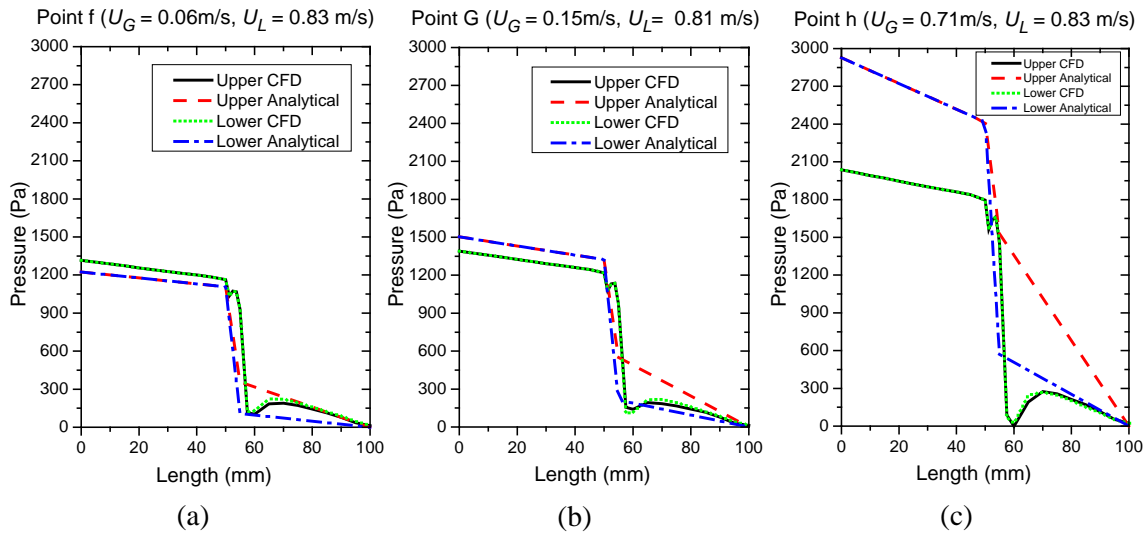

| (a) | (b) | (c) |

Figure 6. Comparison of pressure drop in distributor at point f, g, and h
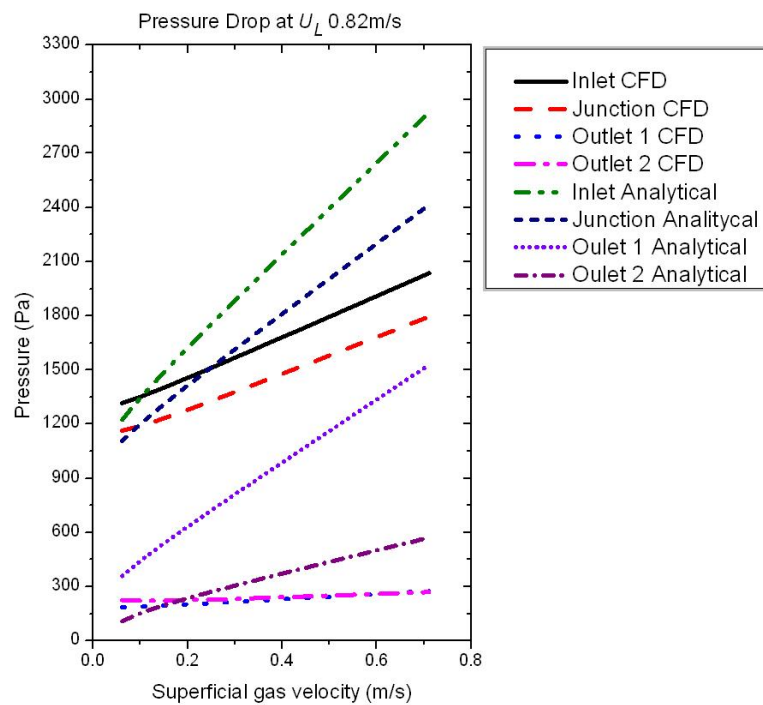

Figure 7. Relationship between pressure drop and superficial gas velocity for $U_L = 0.82$ m/s

6. CONCLUSIONS

The basic study of two-phase flow pattern and pressure drop in a distributor by using air and water as working fluids were presented. There is a small difference of the flow pattern in distributor between

experiment and CFD approach that affect to the two-phase flow deviation ratio. The two-phase flow deviation of the experiment and CFD showed small difference for the water and large difference for the air. The descriptions of flow pattern by experiment and numerical are agreed well with the flow pattern on Mandhane (1974) and Baker (1954) flow pattern map. There are some differences in the pressure drop between analytical model and CFD approach and they are increases with the increasing of superficial gas velocity. The pressure drop increases proportional to superficial gas velocity along the distributor tubes. The pressure drop at branching part of the distributor is biggest, because of sudden enlargement and contraction in branch.

7. REFERENCES

Azzopardi, B. J. 2010, *Multiphase Flow, Chemical Engineering and Chemical Process Technology*, Volume 1, EOLSS Publishers, UK.

Baker, O. 1954. Design of pipe lines for simultaneous flow of oil and gas, *Oil and Gas Journal*, 53: 185-195.

Bell, Stephanie. 2001, *A Beginner's guide to uncertainty of measurement* (Issue 2), National Physical Laboratory, UK

Brennen, C.E. 2005, *Fundamentals of Multiphase Flows*, Cambridge University Press, UK.

Ghajar, A.J. 2005, Non-boiling heat transfer in gas-liquid flow in pipes-a tutorial, *Journal of the Brazilian Society of Mechanical Science and Engineering*, 27(1):46-73.

Ghajar, A.J., Tang, C.C. 2010, Void fraction and flow patterns of two-phase flow in upward and downward vertical and horizontal pipes, *Advances in Multiphase Flow and Heat Transfer*, 4: 232-267.

Ghiaasiaan, S. M. 2008. *Two-Phase Flow, Boiling and Condensation (In Conventional and Miniature Systems)*, Cambridge University Press, UK.

Kandlikar, S. G., Shoji, M., Dhir, V. K. 1999, *Handbook of Phase Change: Boiling and Condensation*, Taylor and Francis, USA.

Lombardi, C., Cassana, C.G. 1992, Dimensionless pressure drop correlation for two-phase mixtures flowing up flow in vertical ducts covering wide parameter ranges, *Heat and Technology*, 10(1-2): 125-141.

Mandhane, J.M., Gregory, G.A., Aziz, K. 1974. A flow pattern map for gas-liquid flow in horizontal pipes, *International Journal of Multiphase Flow*, 1(4):537-553.

Massoud, M. 2005. *Engineering Thermo Fluids (Thermodynamics, Fluid Mechanics, and Heat Transfer)*, Springer-Verlag Berlin Heidelberg, Germany.

Moffat, R.J. 1988, Describing the Uncertainties in Experimental Results, *Experimental Thermal and Fluid Science*, 1(1): 3-17.

Saba, N., Lahey, Jr..R.T. 1984, The analysis of phase separation phenomena in branching conduits, *International Journal of Multiphase Flow*, 10(1): 1-20.

Saisorn, S., Wongwises, S. 2008, Flow pattern, void fraction and pressure drop of two-phase air-water flow in a horizontal circular micro-channel, *Experimental Thermal and Fluid Science*, 32(34):748-760.

Theilacker, J.C., Rode, C.H. 1987, An investigation into flow regimes for two-phase helium flow, *International Cryogenic Materials Conference and Cryogenic Engineering Conference,* USA.

Tong, L. S., Tang, Y. S. 1997, *Boiling Heat Transfer and Two-Phase Flow*, second ed., Taylor and Francis, USA.

Wambsganss, M. W., Jendrzejczyk, J. A., France, D. M. 1991, Two-phase flow patterns and transitions in a small, horizontal, rectangular channel, *International Journal of Multiphase Flow*, 17(3): 327-342.

Wong, T.N., Yau, Y.K. 1997, Flow patterns in two-phase air-water flow, *International Communications in Heat and Mass Transfer*, 24(1): 111-118.

Wongwises, S., Pipathattakul, M. 2006, Flow pattern, pressure drop and void fraction of two-phase flow gas-liquid in an inclined narrow annular channel, *Experimental Thermal and Fluid Science*, 30(4): 345-354.

Yang, C.Y., Shieh, C.C. 2001, Flow pattern of air-water and two-phase R-134a in small circular tubes, *International Journal of Multiphase Flow*, 27(7): 1163-1177.

Yoshioka, S., Kim, H., Kasai, K. 2008, Performance Evaluation and Optimization of A Refrigerant Distributor for Air Conditioner, *Journal of Thermal Science and Technology*, 3(1): 68-77.

Zivi, S.M. 1964, Estimation of steady-state steam void fraction by means of the principle of minimum entropy production, *Journal of Heat Transfer*, 86(2): 247-252.